Received: 22 December 2016 | Revised: 15 March 2017 | Accepted: 18 April 2017

DOI: 10.1002/bio.3353

WILEY LUMINESCENCE
The Journal of Biological and Chemical Luminescence

RESEARCH ARTICLE

Zero and second-derivative synchronous fluorescence spectroscopy for the quantification of two non-classical β-lactams in pharmaceutical vials: Application to stability studies

Eman S. Elzanfaly[1] | Rania M. Youssif[2] | Nahla N. Salama[2] | Ahmed S. Fayed[1] | Hassan A.M. Hendawy[2] | Maissa Y. Salem[1]

[1] Department of Analytical Chemistry, Faculty of Pharmacy, Cairo University, Cairo, Egypt

[2] National Organization for Drug Control and Research (NODCAR), Giza, Egypt

Correspondence
Rania M. Youssif, National Organization for Drug Control And Research (NODCAR), Giza, Egypt.
Email: dr.ronica81@yahoo.com

Abstract

The formation of metal chelates with various ligands may lead to the production of fluorescent chelates or enhance the fluorescence of the chelating agent. This paper describes two sensitive, selective and computer-solved methods, namely, zero order (SF) and second-derivative synchronous spectrofluorimetry (SDSFS) for nano-quantitation of two carbapenems; meropenem (MP) and ertapenem (EP). The methods are based on the chelation of MP with Tb^{3+} and EP with Zr^{4+} in buffered organic medium at pH 4.0 to produce fluorescent chelates. In the zero order method, the relative synchronous fluorescence intensity is measured at 327.0 nm at $\Delta\lambda$ = 70.0 and 100.0 nm for MP and EP, respectively. The second method utilizes a second-derivative technique to enhance the method selectivity and emphasize a stability-indicating approach. The peak amplitudes (^2D) of the second-derivative synchronous spectra were estimated to be 333.06 and 330.06 nm for MP and EP, respectively. The proposed synchronous spectrofluorimetric methods were validated according to the *International Conference on Harmonization* (ICH) guidelines and applied successfully for the analysis of MP and EP in pure forms, pharmaceutical vials and in synthetic mixtures with different degradants of both drugs. Under optimum conditions, the mole-ratio method was applied and the co-ordination ratios of MP–Tb^{3+} and EP–Zr^{4+}chelates were found to be 1:1 and 1:3. The formation constants for the chelation complexes were evaluated using the Benesi–Hildebrand's equation; the free energy change (ΔG) was also calculated. The results indicated that EP–Zr^{4+} was more stable than the MP–Tb^{3+} chelate. Moreover, the developed methods were found to be selective and inexpensive for quantitative determination of both drugs in quality control laboratories at nano-levels.

KEYWORDS

derivative synchronous spectrofluorimetry, ertapenem, meropenem, nano-determination, stability-indicating

1 | INTRODUCTION

Meropenem (MP) (Figure 1): (4R,5S,6S)-3-[(3S,5S)-5-(dimethylcarbamoyl)-3-pyrrolidinyl]thio]-6-[(1R)-1-hydroxyethyl]-4-methyl-7-oxo-1-azabicyclo[3.2.0] hept-2-ene-carboxylic acid, trihydrate[1]; and ertapenem (EP) (Figure 1): (1R, 5S, 6S, 8R, 2′S, 4′S)-2-(2-(3-carboxyphenylcarbamoyl)pyrrolidin-4–4ylthio)-6-(1-hydroxyethyl)-1-methylcarbapenem-3-carboxylic acid (sodium salt)[2], are non-classical β-lactam antibiotics (Carbapenems), having ultra-broad antibacterial spectrum.[3,4]

The literature survey comprised several analytical methods for quantitative determination of (MP) and (EP). These methods include spectrophotometry[5,6], capillary zone electrophoresis (CZE)[7], high performance liquid chromatography (HPLC)[8–22], micellar

Abbreviations used: GCE, graphene composite modified electrodes; FTIR, Fourier transform infrared spectroscopy; HPLC, high performance liquid chromatography; ICH, International Conference on Harmonization; LOD, limit of detection; LOQ, limit of quantification; MS, mass spectroscopy; RSD, relative standard deviation; SD, standard deviation; SDSFS, second-derivative synchronous fluorescence; SF, synchronous fluorescence.

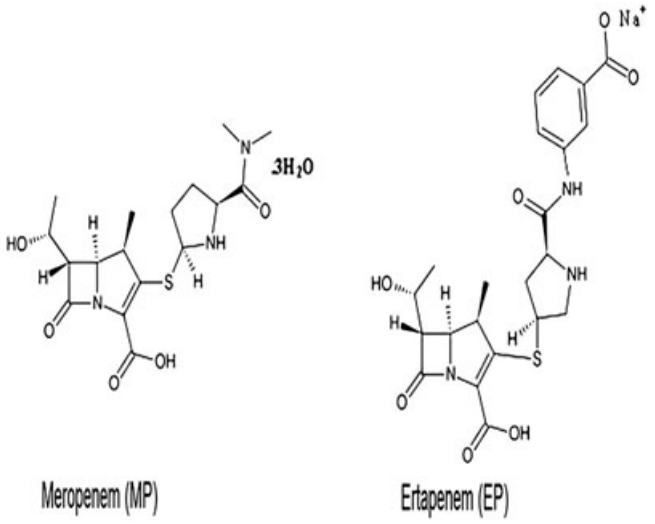

FIGURE 1 Chemical structures of meropenem (MP) and ertapenem (EP)

electrokinetic capillary chromatography[19] and thin layer chromatography (TLC)[9,15]; square wave and adsorptive anodic stripping voltammetric methods were previously investigated.[23]

The determination of doripenem and meropenem metabolites using polyaniline and graphene composite modified electrodes (GCE) and diamond electrodes was performed.[24,25] In these studies the effect of different supporting electrolytes and different pH values were investigated.

Synchronous spectrofluorimetry (SF) is more advantageous than conventional fluorescence spectroscopy due to the sharper and narrower spectra obtained upon application. This results in simpler spectra, low interference and high selectivity, which permits the resolution of overlapping spectra and effectiveness for achieving data for quantitative determination. The method is more valuable than differentiation of the conventional emission spectrum in terms of sensitivity, because the amplitude of the derivative signal is inversely proportional to the band width of the original spectrum.[26–31] It has been used for multi-component analysis[32,33] and for the determination and characterization of inorganic semiconductor nanocrystals.[34]

The aim of this study was the nano-sensitive determination of MP and EP in their pure forms and pharmaceutical vials. Synchronous fluorescence (SF) aided in baseline correction of the blank reagents solutions that were difficult to be omitted by conventional fluorimetry. The relative fluorescence intensity of the studied drugs was greatly affected in the presence of their corresponding hydrolytic and oxidative degradants. Such a problem was resolved by second-derivative synchronous fluorescence (SDSFS). Thus, the proposed derivative method could be considered as a stability-indicating method for the determination of MP and EP with satisfied accuracy and precision.

To the best of our knowledge, no spectrofluorimetric method in the nano-range has been yet reported for the determination of MP and EP, neither in pure forms nor in pharmaceutical preparations. Also, no fluorimetric method has been reported as a stability study. In addition, the hydrolytic and oxidative degradants of the studied drugs were identified by infrared spectroscopy and mass spectrometry, and the pathways of degradation were illustrated.

2 | EXPERIMENTAL

2.1 | Apparatus

The fluorescence spectra and measurements were recorded using a Cary Eclipse fluorescence spectrophotometer (Agilent Technologies, Australia), equipped with a 150 W xenon arc lamp. The slit width for excitation and emission was set at 5.0 nm, scan rate at medium (600 nm/min) and the photomultiplier detector voltage was set to high. A 1-cm quartz cuvette was used. Derivative spectra were computed using filter size 25 at 2.0 nm intervals with Cary Eclipse software, scan application, version 1.2 (147) (Agilent Technologies, Australia). The pH measurements were carried out using a digital pH-meter (Jenway 3310 UK) with a combined glass electrode. Fourier transform infrared spectroscopy (FTIR; IR Prestige 21, Shimadzu, Japan) was used. A GC/MS-QP1000EX quadruple mass spectrometer (Shimadzu-Japan) equipped with an electron multiplier detector was used for recording MS spectra.

2.2 | Chemicals and reagents

Meropenem trihydrate (99.9% on anhydrous basis) was kindly provided by Sumitomo Pharmaceuticals Co. Ltd, Japan. Meronem® vials (1140.0 mg of meropenem trihydrate) were manufactured by AstraZeneca, UK. Ertapenem, certified to be 100.1% as the sodium salt, was kindly supplied by Merck & Co., USA. Invanz® vials (1046.0 mg as ertapenem sodium) were manufactured by MSD, USA.

Terbium (III) chloride hexahydrate ($TbCl_3 \cdot 6H_2O$), Acros Organics, USA, zirconium dichloride oxide octahydrate (Alfa Aesar GmbH & Co. KG, Germany), Tris buffer, 1-butanol and 1-propanol (Sigma-Aldrich, USA), methanol (Labscan, Poland), acetonitrile and 2-propanol (SD Fine Chemicals Limited, India), sodium chloride, ascorbic acid, uric acid and anhydrous glucose (ADWIC, Egypt), sodium hydroxide (LOBA Chemie, India), hydrochloric acid 37% (Honeywell, Germany), acetone (TEDIA, USA), absolute ethanol (Riedel-de Hein, USA) and hydrogen peroxide, 30% *v*/v (Panreac, Spain) were used in this study. All chemicals, solvents and reagents used throughout this work were of analytical grade.

$TbCl_3$ (1.0×10^{-3} M) and $ZrOCl_2$ (4.0×10^{-3} M) solutions were prepared by dissolving them in water. Tris buffer solution was prepared over the pH range of 2.0–9.0[35], the pH of the solutions was adjusted by adding 1.0 M NaOH or 1.0 M HCl and then diluted to 200 ml with water. Bi-distilled water was used throughout the whole work and is indicated by the word 'water'.

2.3 | Standard solutions

2.3.1 | Standard solutions of MP and EP

Stock standard solutions of 100.0 μg/ml concentration were prepared by accurately weighing 11.4 and 10.5 mg of each of MP and EP certified materials (equivalent to 10 mg anhydrous base of MP or free acid of EP), respectively in 100 ml water. Working standard solutions 10.0 μg/ml were prepared by transferring 10 ml of stock solutions into two separate 100-ml volumetric flasks. The solutions were freshly prepared on the day of analysis.

2.3.2 | Standard solutions of hydrolytic and oxidative degradants

Hydrolytic degradants (acid or alkaline) of MP and EP were prepared by mixing 11.4 and 10.5 mg, respectively, with either 10.0 ml of HCl or NaOH (0.5 M, each), then set aside for 1 h. The solutions were neutralized with previously calculated NaOH or HCl (0.5 M, each) as appropriate. Oxidative degradants were prepared by adding 10 ml of 3.0% and 6.0% (v/v) H_2O_2 to MP and EP, respectively, and set aside for 30 min. All prepared degradants were evaporated on a thermostatic water bath to dryness. The collected degradants' residues were dissolved in methanol, filtered and evaporated under vacuum. They were further used for their structure elucidation using FTIR and MS spectra (illustrated below). For preparation of stock standard solutions, the same procedure was followed and each degradant's residue was dissolved in 100 ml water, separately, to obtain a final concentration 100.0 μg/ml. The solutions were diluted each with water to reach a 10.0 μg/ml concentration as working degradant solutions of the studied drugs.

2.4 | General procedures

2.4.1 | SF procedure for MP and construction of calibration plot

Aliquots of MP working standard solution (10.0 μg/ml) over the concentration range 1.0–6.0 μg/ml were accurately transferred into a series of 10-ml volumetric flasks and the solutions were diluted to the mark with water and mixed well. One ml of each of the prepared solutions was transferred into a series of 10-ml volumetric flasks followed by 1.0 ml of Tb^{3+} (1.0×10^{-3} M), 1.0 ml of Tris buffer (pH 4.0), then completed to mark with methanol and mixed well. The solutions were set aside for 30 min for completion of reaction. The obtained final solutions were in the range 100.0–600.0 ng/ml. The SF spectra were recorded for the prepared solutions in the wavelength range 250.0–450.0 nm by scanning at wavelength intervals Δλ = 70.0 nm and a scan rate of 600 nm/min using 5.0 nm excitation and emission slits. The relative fluorescence intensity (ΔFI) was measured at 327.03 nm and plotted against the final drug concentration in ng/ml to obtain the calibration plots. The regression equation was computed.

2.4.2 | SF procedure for EP and construction of calibration plot

Aliquots of EP working standard solution (10.0 μg/ml) over the concentration range 0.5–7.0 μg/ml were accurately transferred into a series of 10-ml volumetric flasks and the solutions were diluted to the mark with water and mixed well. One ml of each of the previously prepared standard solutions of EP was further transferred into a series of 10-ml volumetric flask followed by 1.0 ml of Zr^{4+} (4.0×10^{-3} M) reagent solution, 1.0 ml of Tris buffer (pH 4.0), completed to mark with 2-propanol and mixed well. The solutions were set aside for 10 min for completion of reaction. The obtained final solutions were in the range 50.0–700.0 ng/ml. The SF spectra were recorded for the prepared solutions under the same parameters as mentioned at 2.4.1., but using Δλ = 100.0 nm. The relative fluorescence intensity (Δ FI) was measured at 327.03 nm and plotted against the final drug concentration in ng/ml to obtain the calibration plot. The regression equation was computed.

2.4.3 | SDSFS procedure for MP and EP and construction of calibration plots

SF spectra of solutions of the MP–Tb^{3+} and EP–Zr^{4+} fluorescent chelates obtained were computed to obtain second-derivative spectra using filter size 25 at 2.0 nm interval and Cary Eclipse software. MP was selectively measured at 333.06 nm, whereas EP could be determined at 330.06 nm (zero crossing for hydrolytic and oxidative degradants) in the recorded second-derivative synchronous fluorescence spectra (SDSFS). The peak amplitudes (^2D) of the second-derivative spectra were plotted against final drug concentrations (ng/ml) to obtain the calibration plot. Alternatively, the corresponding regression equations were derived.

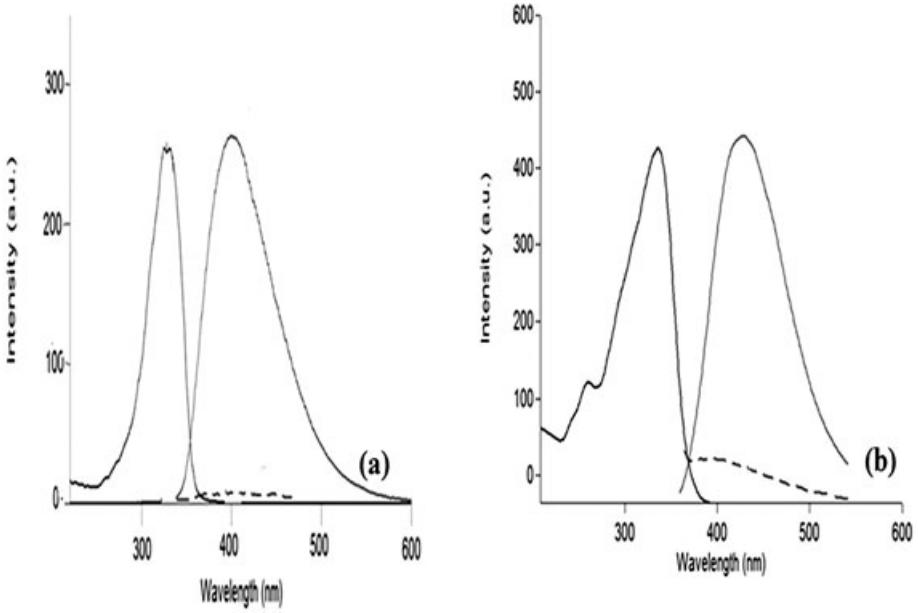

FIGURE 2 Fluorescence excitation and emission spectra of MP–Tb^{3+} (a) and EP–Zr^{4+} (b) fluorescent chelates against blanks reagents solutions (----) at pH 4.0 [MP], [EP] = 5.0 μg/ml

2.5 | Applications

2.5.1 | Analysis of MP and EP in their pharmaceutical vials

The contents of five vials of Meronem or Invanz pharmaceutical vials (1.0 gm/vial) were accurately weighed and mixed, separately. A weight of 13.5 and 12.5 mg equivalent to 10 mg anhydrous base of MP or free acid of EP were quantitatively transferred into two separate 100.0-ml volumetric flasks and then dissolved in water. Ten ml of each drug was transferred into 100.0-ml volumetric flasks. Aliquots of 2.0 and 5.0 ml of these solutions for MP and EP, respectively, were successively transferred into two sets of 10-ml volumetric flasks and diluted with water. The SF procedures of MP or EP were then applied. The nominal content of the vials was determined either from the previously plotted calibration plots or using the corresponding regression equations.

2.5.2 | Analysis of laboratory prepared mixtures with hydrolytic /oxidative degradants

Aliquots of MP, EP and their hydrolytic or oxidative degradants working solutions in different ratios (1–50%) were transferred into a series of 10-ml volumetric flask, diluted to mark with water and mixed well. SDSFS procedure for MP or EP was then computed. The percentage recoveries were calculated by referring to the calibration plots, or using the corresponding regression equations.

3 | RESULTS AND DISCUSSION

3.1 | Spectral characteristics

Tb^{3+} is one of the lanthanides that exhibit fluorescence with a sensitivity can be improved by chelation through energy transfer from ligands.[36] Conversely; Zr^{4+} was used in the formation of a fluorescent chelate that was previously reported for the determination of quinolones.[37,38] Upon chelation with fluoroquinolones, Zr^{4+}produces highly stable fluorescent chelates.[37] This may be attributed to the rigidity of the formed complex molecular structure. Both MP and EP exhibited a normal fluorescence with Tb^{3+} and Zr^{4+} at λ_{em} 400.0 and 430.0 nm using λ_{ex} 325.0 and 336.0 nm for MP and EP, respectively (Figure 2). The zero order fluorescence spectra of both drugs overlapped considerably with the fluorogenic reagents blanks and, thus, conventional spectrofluorimetry was not possible for the determination of these drugs. This fluorescence was exploited to develop zero order SF for baseline correction of blank reagents and thus, nano-determination of the studied drugs was achieved.

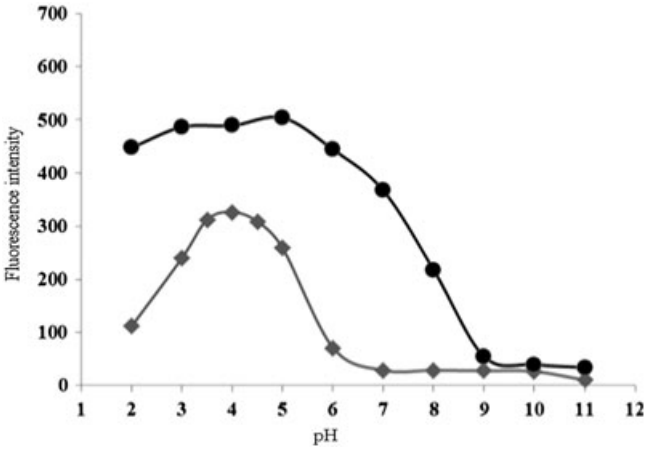

FIGURE 4 Influence of different pH on the fluorescence intensity of MP-Tb^{3+} (♦) and EP–Zr^{4+} (●) fluorescent chelates. [MP], [EP] = 1.0 μg/ml, λ_{ex} of 325.0 and 336.0 nm, λ_{em} of 400.0 and 430.0 nm; methanol and 2-propanol as diluting solvents

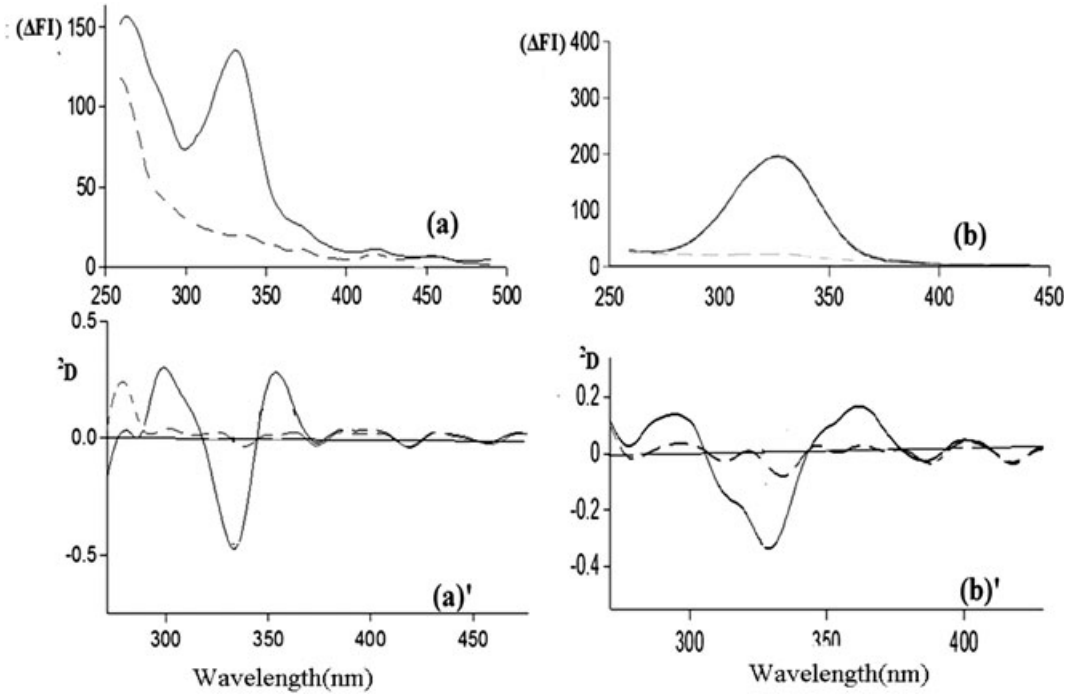

FIGURE 3 The zero order (a, b) and second-derivative (a´, b´) synchronous fluorescence spectra of fluorescent chelates of (a) MP–Tb^{3+} (—) and its hydrolytic or oxidative degradants (– – -); and (b) EP–Zr^{4+} (—) and its degradants (– – -) at pH 4.0 and Δλ = 70 and 100 nm, respectively. [MP] = 200.0 ng/ml, [EP] = 100.0 ng/ml

Derivative spectrofluorimetry, based on mathematical transformation of the zero order curves into the derivative spectra can overcome overlapping problems.[39] This led us to adopt second-derivative synchronous fluorescence spectroscopy technique (SDSFS) as a stability-indicating methodology.

The zero order and SDSFS spectra of each MP–Tb^{3+} and EP–Zr^{4+} and their hydrolytic or oxidative degradants (a, a´) and (b, b´) respectively are given in Figure 3. The spectra of both hydrolytic and oxidative degradants are nearly the same, as shown in Figure 3. The figure shows that the hydrolytic and oxidative degradants had no spectrofluorimetric characteristics and almost plateau spectra were obtained for different degradants. This facilitated the determination of each drug at the zero crossing point of its corresponding degradant. These wavelengths were 333.06 for MP and 330.06 nm for EP.

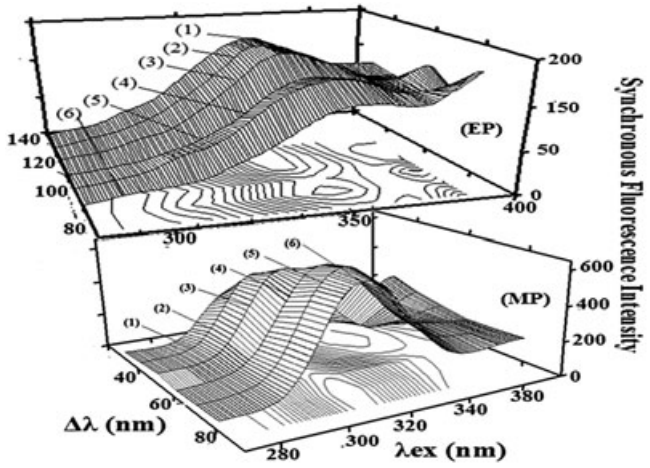

FIGURE 5 Three-dimensional and two-dimensional (contour plots) of total synchronous fluorescence spectra showing the effect of constant wavelength difference (Δλ) on synchronous fluorescence spectra of MP at (1) 30, (2) 40, (3) 50, (4) 60, (5) 70, (6) 80, and of EP at (1) 90, (2) 100, (3) 110, (4) 120, (5) 130, (6) 140, respectively

3.2 | Optimization of experimental parameters

The effect of different experimental conditions affecting fluorescence intensities: metal ion concentration, pH, reagents order of addition, time of reaction, diluting solvents, and delta lambda of the studied drugs were carefully studied and optimized. Such factors were changed individually while others were kept constant.

3.2.1 | Influence of metal (Tb^{3+}, Zr^{4+}) ions concentration

Different concentration ranges of Tb^{3+} (0.2–1.2 × 10^{-3} M) and Zr^{4+} (0.5–6.0 × 10^{-3} M) reagents solutions were studied for the fluorescence intensity of MP and EP, respectively. It was found that 1.0 ml of each of 1.0 × 10^{-3} M of Tb^{3+} and 4.0 × 10^{-3} M of Zr^{4+} was appropriate for producing maximum fluorescence intensities for both drugs.

3.2.2 | Influence of different pH

The maximum fluorescence intensities of the drug solutions were studied by varying the pH of Tris buffer in the range pH 2.0–11.0 while keeping other experimental factors constant. At high pH, fluorescence quenching occurs. However, when the pH was further decreased, the intensity of fluorescence was enhanced sharply. So, the choice of pH 4.0 (slightly acidic medium) was crucial for obtaining maximum and stable fluorescence enhancement of both drugs, as shown in Figure 4.

3.2.3 | Reagents addition order and time stability test

The effect of the order of reagents addition on the fluorescence intensity was studied. The results showed that an addition order of the used drug, Tb^{3+}/Zr^{4+} and Tris buffer (pH 4.0), offered the optimal fluorescence intensity, therefore, this order of addition described above in the general procedure, was chosen for application. The stabilities of the formed MP–Tb^{3+} and EP–Zr^{4+} fluorescent chelates were studied. The fluorescence emission measurement of both drugs attained constancy and reached maximum in 30 min for MP and 10 min for EP after all reagents had been added. They remained stable for more than 1 h.

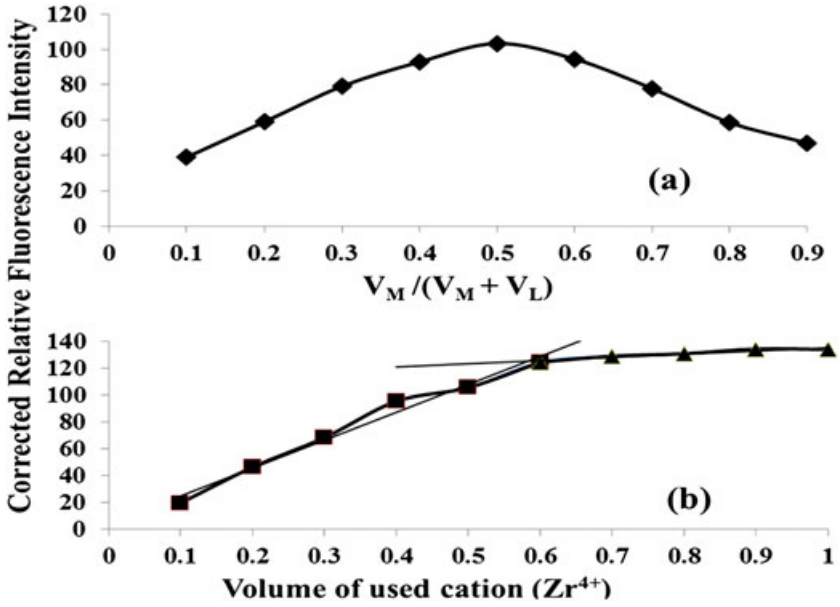

FIGURE 6 (a) Job's method for continuous variation for MP (1.0 × 10^{-3} M) with Tb^{3+} (1.0 × 10^{-3} M). (b) the mole-ratio method for EP (0.2 ml of 4.0 × 10^{-3} M) with different volumes of Zr^{4+} (4.0 × 10^{-3} M)

3.2.4 | Selection of optimal wavelength interval Δ λ

The optimum Δλ value is a crucial factor that affects the SF scanning technique concerning resolution, sensitivity, and features. It can directly influence spectral shape, bandwidth, and signal value. For this reason, a wide range of Δλ (30–140 nm) was examined. Wavelength intervals Δλ of 70 and 100 nm were chosen as optimal for baseline correction of blank reagents solutions as they are well known as fluorogenic ions. These Δλ values were chosen as they resulted in a zero-ing baseline, the good shape SF spectra with the highest intensity values as shown in Figure 5. Lower and higher Δλ values than the optimum

TABLE 1 Performance data for meropenem and ertapenem by the proposed SF and SDSFS methods

Regression equation parameters	Meropenem		Ertapenem	
	SF	SDSFS	SF	SDSFS
Linearity and range (ng/ml)	100.0–600.0	100.0–600.0	50.0–700.0	50.0–700.0
Slope (b)	0.2627	−0.00125	0.1754	−0.00119
Intercept (a)	51.338	−0.2158	52.859	−0.21579
Correlation coefficient	0.9998	0.9985	0.9997	0.99899
SD of slope	6.344×10^{-3}	8.23×10^{-5}	4.525×10^{-3}	6.364×10^{-5}
SD of intercept	2.475	0.01308	0.6702	0.0094
$S_{y/x}$	1.08522	0.014055	0.99603	0.01398
LOD (ng/ml)	31.0	34.54	12.6	25.85
LOQ (ng/ml)	94.0	104.6	40.0	58.33

ΔFI or ^2D = a + bc, ΔFI = relative fluorescence intensity while ^2D is the second-derivative value, a = intercept, b = slope, C = concentration in ng/ml, $S_{y/x}$ = standard deviation of residuals, LOD = limit of detection, LOQ = limit of quantitation.

TABLE 2 Statistical comparison for the results obtained by the proposed SF, SDSFS and comparison methods[2,45] for the analysis of meropenem and ertapenem in pure forms

Items	Meropenem			Ertapenem		
	SF method	SDSFS method	Official method[2]	SF method	SDSFS method	Reported method[45]
Mean[a]	100.11	99.47	100.18	99.11	99.86	100.22
± SD	1.460	1.295	1.322	0.826	1.129	1.312
%RSD	1.458	1.302	1.319	0.833	1.131	1.309
SE	0.652	0.579	0.591	0.3694	0.505	0.586
%REr	± 0.652	± 0.582	± 0.589	± 0.373	± 0.506	± 0.585
n	5	5	5	5	5	5
Variance	2.131	1.678	1.747	0.682	1.275	1.721
t-test	0.076	0.384	(1.860)	1.605	0.208	(1.860)
F-test	1.220	1.041	(6.390)	2.523	1.350	(6.390)

SD = standard deviation, %RSD = per cent relative standard deviation, SE = standard error, %REr = percent relative standard error, the values in parenthesis are the corresponding theoretical values of *t* and F at *P* = 0.05.

[a]Average of five determinations.

TABLE 3 Intraday and intermediate precision data of meropenem and ertapenem in pure forms by the proposed SF and SDSFS methods

Parameter	Concentration of meropenem in ng/ml						Concentration of ertapenem in ng/ml					
	300.0		400.0		500.0		200.0		400.0		600.0	
	SF	SDSFS	SF	SDSFS	SF	SDSFS	SF	SDSFS	SF	SDSFS	SF	SDSFS
Intraday												
Mean[a]	100.7	99.69	101.2	101.89	101.3	100.62	99.56	98.59	98.36	98.20	100.10	100.89
±SD	1.380	0.533	1.234	0.196	0.988	0.036	0.412	0.144	0.265	0.100	0.655	0.290
% RSD	1.369	0.535	1.219	0.193	0.975	0.035	0.414	0.146	0.269	0.102	0.654	0.287
% REr	0.790	0.309	0.704	0.111	0.563	0.021	0.239	0.085	0.155	0.059	0.378	0.166
Variance	1.904	0.284	1.523	0.038	0.976	0.001	0.170	0.021	0.070	0.010	0.429	0.084
Intermediate precision												
Mean[a]	99.98	99.23	101.0	101.5	100.3	98.46	100.2	100.38	100.9	100.53	101.1	99.42
±SD	1.750	0.126	0.573	0.265	1.320	0.191	1.950	1.306	1.429	1.858	0.685	1.636
% RSD	1.749	0.127	0.567	0.261	1.316	0.194	1.947	1.301	1.416	1.848	0.677	1.645
% REr	1.010	0.073	0.327	0.150	0.760	0.112	1.124	0.751	0.818	1.839	0.391	0.950
Variance	3.062	0.016	0.328	0.070	1.742	0.036	3.803	1.707	2.042	3.453	0.470	2.676

[a]Average of three determinations.

TABLE 4 Determination of meropenem and ertapenem in their pharmaceutical vials by the proposed SF and SDSFS methods and application of the standard addition technique

Pharmaceutical vial	% found ± SD[a]		Standard addition technique			Pharmaceutical vial	% found ± SD[a]		Standard addition technique		
				% recovery [a]					Added (ng/ml)	% recovery[a]	
	SF	SDSFS	Added (ng/ml)	SF	SDSFS		SF	SDSFS		SF	SDSFS
Meronem ® vial B.N.: KF458 (200.0 ng/ml)	100.44 ± 1.710	100.59 ± 0.703	100.0	98.0	98.0	Invanz ® vial B.N.: 2186310 (200.0 ng/ml)	100.09 ± 1.660	99.85 ± 1.285	100.0	98.12	101.70
			200.0	100.54	100.33				200.0	102.0	101.40
			300.0	102.0	101.60				300.0	98.47	99.34
			400.0	98.26	98.55				400.0	101.11	100.27
									500.0	101.79	99.90
Mean ± %RSD			99.70 ± 1.917		99.62 ± 1.659	Mean ± %RSD			100.29 ± 1.856		100.52 ± 0.995

[a]Average of three determinations.

TABLE 5 Determination of meropenem and ertapenem in presence of their corresponding hydrolytic and oxidative degradants by the proposed SF and SDSFS methods

% of added degradants	Meropenem (recovery of intact drug[a]%)				Ertapenem (recovery of intact drug[a]%)			
	Hydrolytic degradant		Oxidative degradants		Hydrolytic degradant		Oxidative degradants	
	SF	SDSFS	SF	SDSFS	SF	SDSFS	SF	SDSFS
1	99.27	99.80	101.96	100.00	98.04	99.20	100.63	101.70
2	100.74	100.70	100.37	99.68	100.18	99.60	99.52	101.10
5	101.35	101.40	98.23	98.22	98.88	99.53	102.00	101.13
10	101.54	101.81	–	99.11	101.92	100.45	100.31	99.63
20	101.89	101.60	–	100.04	98.23	100.60	99.40	101.10
25	–	100.49	–	101.48	100.21	99.90	99.72	100.86
50	–	102.00	–	101.96	–	99.50	–	101.10
Mean ± %RSD	100.08 ± 0.962	101.14 ± 0.795	101.16 ± 1.111	100.07 ± 1.294	99.58 ± 1.484	99.83 ± 0.522	100.08 ± 0.784	100.95 ± 0.628

[a]Average of three determinations.

values showed low fluorescence intensity for both compounds. However, very low and very high Δλ values caused irregularities in the spectral shape.

3.2.5 | Effect of diluting solvents

Dilution with different diluents such as water, methanol, ethanol, acetonitrile, Tris buffer (pH 4.0), acetone, 2-propanol and 1-propanol was attempted. It was found that the fluorescence intensity was maximal in methanol and 2-propanol more than in other diluents, therefore methanol and 2-propanol were selected as the diluents of choice in this study for MP and EP, respectively.

3.3 | Determination of coordination ratio and calculation of formation constants

Job's method for continuous variation and the mole-ratio method were used to determine the coordination ratio of MP–Tb^{3+} and EP–Zr^{4+}, as shown in Figure 5(a) and 5(b), respectively. The results indicated that the MP–Tb^{3+}coordination ratio was 1:1, while that for EP–Zr^{4+} was 1:3, forming fluorescent chelates (Figure 6).

Formation constant K_f of the reaction product was calculated by the Benesi–Hildebrand's method[40], according to the following equation 1:

$$K_f = \frac{F/F_m}{\left[(1-F/F_m)^{n+1}\right] c^n n^n} \quad (1)$$

where F and F_m are the observed maximum fluorescence and the fluorescence obtained from the extrapolation of the two lines obtained from the mole-ratio method, respectively; *n* is the mole fraction of the reagent (the ratio is 1:1 in case of Tb^{3+} therefore, *n* = 0.5; and 3:1 for Zr^{4+}, so *n* = 0.6); C, is the molar concentration of the drug used in the mole-ratio method. Using the above equation, K_f was found to be 2.111 × 10^3 and 8.62 × 10^3 L/mol using Tb^{3+} and Zr^{4+} respectively. Gibbs free energy changes (ΔG) were also calculated according to the following equation 2:[41]

$$\Delta G = -2.303RT \log K_f \quad (2)$$

where R = gas constant = 8.314 Joule/degree/mole; T = absolute temperature = °C + 273, Using the above equation, ΔG was found to be −1.865 × 10^4, and −2.21 × 10^4 Joule/mole applying Tb^{3+} and Zr^{4+}, respectively. The high free energy (ΔG) indicated the stability of formed fluorescent chelates.[42]

3.4 | Validation of the proposed methods

The methods were tested for linearity, selectivity, accuracy and precision.

3.4.1 | Linearity and range

Under the above-described experimental conditions, calibration plots showed a linear dependence of the relative fluorescence intensity (ΔFI) of Synchronous spectra or the second-derivative peak amplitude (^{2}D) against the drug concentration (ng/ml). The calibration plots show a linear trend over the ranges of 100.0–600.0 and 50.0–700.0 ng/ml at λ of 327.03 nm for zero order SF and at λ of 333.06 and 330.06 nm for SDSFS of both MP and EP, respectively.

Statistical analysis[43] of the data gave high value of the correlation coefficient (r) of the regression equations (Table 1). These data pointed out the low scattering of the points around the calibration curve and high accuracy and precision of the proposed methodology.

3.4.2 | Limit of detection and limit of quantification (LOQ)

The limit of detection (LOD) was determined according to ICH Q2B recommendations[44] by evaluating the minimum level of the analyte that can be readily detected (LOD = 3.3σ/S), where S is the slope of the calibration plot and σ is the standard deviation of the intercept of the regression line. The limit of quantification (LOQ) was determined, below which the calibration graph is non-linear (LOQ = 10σ/S). The results of LOD and LOQ of MP and EP by the proposed techniques are cited in Table 1.

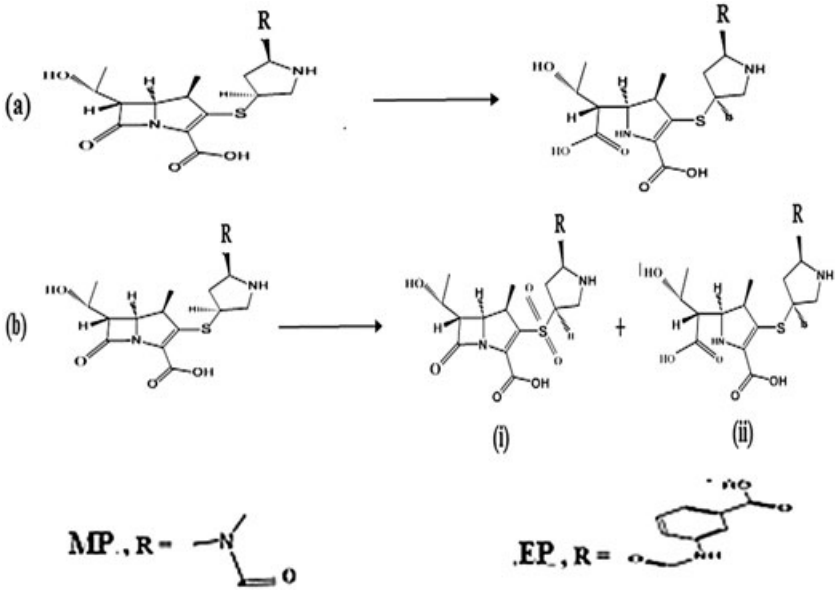

SCHEME 1 General suggested pathways of hydrolytic (a) and oxidative (b)-degradation for MP and EP

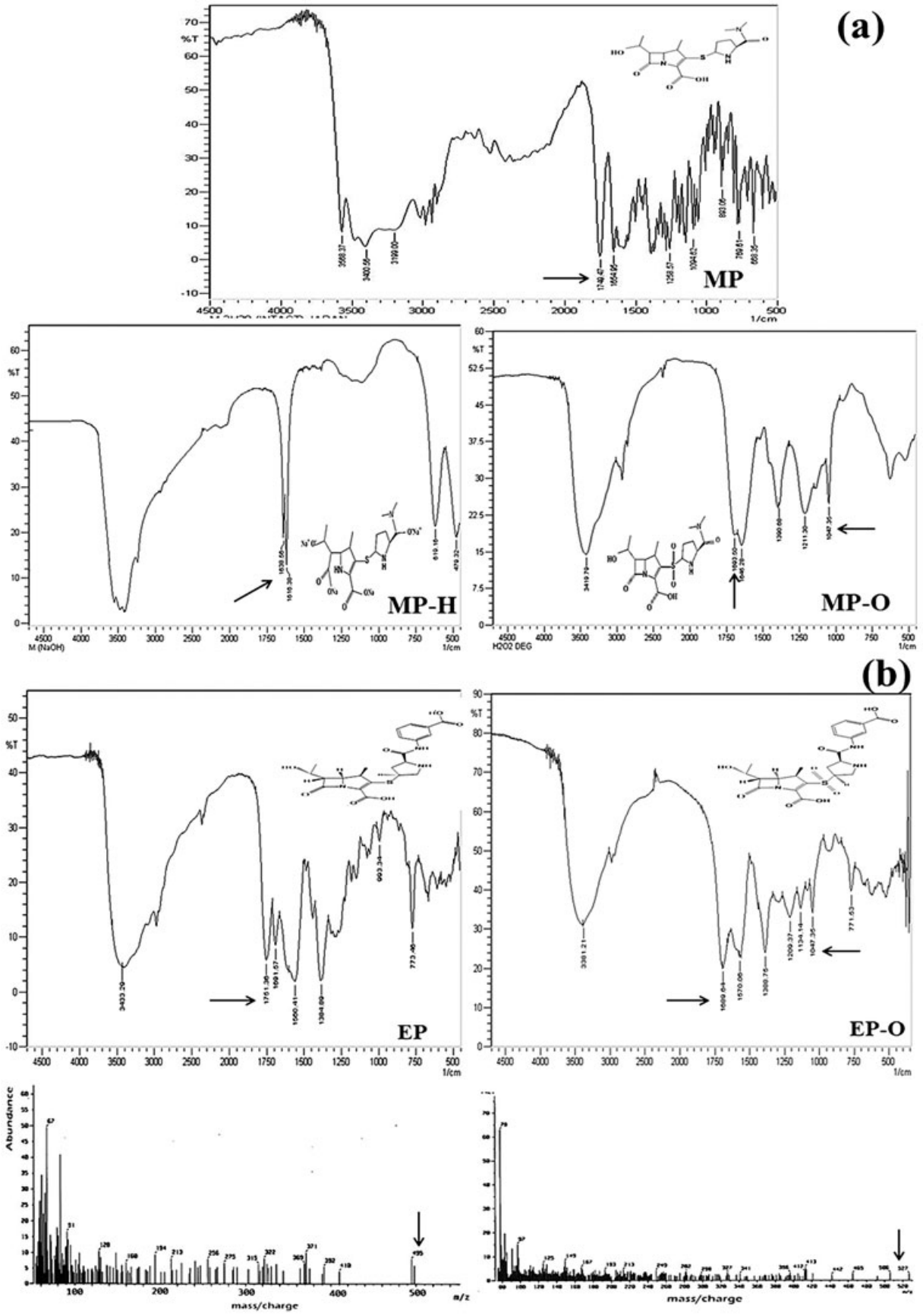

FIGURE 7 (a) FTIR spectra of MP and its hydrolytic (MP–H) and oxidative (MP–O)-degradants. (b) FTIR and MS spectra of EP and its oxidative degradant (EP–O)

3.4.3 | Accuracy

To prove the accuracy of the proposed methods, standard solutions of the studied drugs were analyzed. The results obtained by the proposed methods were favorably compared with those obtained by comparison methods.[2,45]. The percentage recoveries (Table 2).show excellent accuracy. To prove the accuracy of the proposed methods, statistical analysis[43] of the results using Student's *t*-test and variance ratio F-tests, revealed no significant differences between the performances of proposed and reference methods in terms of accuracy and precision (Table 2).

3.4.4 | Precision

Repeatability

The repeatability was evaluated through the replicate analysis of different concentrations of the studied drugs on the same day. The mean percentage recoveries based on the average of three separate determinations are abridged in Table 3.

Intermediate precision

Intermediate precision was obtained through replicate analysis of different concentrations of the studied drugs on 3 successive days. The percentage recoveries are based on the average of three separate determinations. The relative standard deviations were found to be small, indicating reasonable repeatability and intermediate precision of the proposed methods (Table 3).

3.4.5 | Robustness and ruggedness of the proposed methods

The robustness of the procedures adopted was demonstrated by the consistency of the relative fluorescence values with the deliberately minor changes in the experimental parameters such as Tris buffer of pH 4.0 ± 0.2 produced a constant (ΔFI) using Tb^{3+} and Zr^{4+}, respectively. Changing the volume (1.0 ± 0.2 ml) of Tb^{3+} (1.0×10^{-3} M) and Zr^{4+} (4.0×10^{-3} M) ions did not greatly affect the relative fluorescence intensity of the formed fluorescent chelates.

Ruggedness of the proposed methods was confirmed by analyzing five sets of experiments using two different laboratories and different analysts; no significant difference was obtained between the results in this study as %RSD < 2%.

3.5 | Application to pharmaceutical vials

The proposed methods were applied successfully for the determination of MP and EP in their pharmaceutical vials. The concentrations of the drugs were calculated referring to the corresponding regression equations. The results are summarized in Table 4. After testing other constituents as pH adjustors packed in vials such as sodium carbonate and sodium bicarbonate, no interference from the sample matrix was observed on the proposed methods. The results were found to be in good agreement with the labeled amount. The results of the standard addition technique are cited in Table 4.

3.6 | Selectivity and specificity

3.6.1 | Effect of potential interferences

The selectivity of the SF method was investigated by observing vial excipients and other different interference materials. The resulting fluorescence intensity was compared with those obtained for MP and EP at the same concentration. It was found that sodium carbonate, sodium bicarbonate, ascorbic acid, uric acid and glucose did not significantly interfere with the relative fluorescence intensities (ΔFI) of the studied drugs. These matrix components did not show any interfering fluorescence spectral peaks with the studied drugs.

3.6.2 | Analysis of MP and EP in the presence of their hydrolytic or oxidative degradants using the proposed SDSFS method

The SDSFS method was successfully applied to determine MP and EP in the presence of their different degradants presenting a ratio of 50% degradation of the parent drug as stated by ICH guidelines.[44] The peak amplitude values of SDSFS intensities were also measured. The concentrations of the drug were calculated according to the linear regression equations of the calibration plots. The results obtained regarding %RSD was compared with those obtained using HPLC comparable methods.[2,45] The results indicate a high accuracy of the proposed derivative method as shown in Table 5. The obtained high specificity of the developed SF methods for MP and EP was attributable to the mechanism of oxidation of both drugs in relation to the pathways of the hydrolytic and oxidative degradation as well be presented in Scheme 1.

The hydrolytic degradation of non-classical β-lactam drugs[9,15,46] was characterized evenly using FTIR spectroscopy by cleavage of the β-lactam ring carbonyl group at 1750 cm^{-1} to secondary amine and carboxylic group at 1638.5 cm^{-1}, resulting in the formation of an opened ring-degradant in acidic medium and sodium salt degradants in basic medium. The mass spectrum of MP has a m/z of 381 and the alkaline-degradant exhibited new peak at m/z 489.

For oxidative degradation, two different degradants (i and ii) were formed. The first degradant exhibited the characteristic β-lactam carbonyl group at 1690 cm^{-1} with the formation of a sulfone group (O = S = O) at 1047 cm^{-1}; the second degradant was the same as the hydrolytic degradant. The obtained mass spectrum of EP has an m/z of 495 and the oxidative degradants of MP and EP exhibited new peaks at m/z 415 and 527, respectively. Scheme 1(a, b) shows the suggested pathways for hydrolytic and oxidative degradation of the studied drugs.

The obtained hydrolytic and oxidative degradants of both drugs were characterized and elucidated using FTIR and mass spectroscopy (MS) spectra as illustrated in Figure 7(a, b).

4 | CONCLUSION

Analytical laboratories require accurate results, faster and more economically than ever before. The present work describes SF spectroscopy and derivative SF for the nano-determination of two non-classical β-lactam antibiotics, meropenem and ertapenem, in presence

of their different degradation products and in pharmaceutical vials using simple procedures. The methods are based on the chelation of MP with lanthanides (Tb^{3+}) and EP with Zr^{4+} with the formation of fluorescent chelates, which improved the fluorescence through energy transfer from ligands. The results obtained were in good agreement with those obtained by comparison HPLC methods. In the literature, to our knowledge, there is no other spectrofluorimetric method concerned with the analysis of both drugs. Unlike most recommended HPLC procedures, the proposed SF and SDSFS methods are simple, rapid and inexpensive. The procedures applied do not involve any critical reactions or tedious sample preparations. The simplicity and economy of the proposed methods and environmental safety of the used solvents allow their application for routine work in quality control laboratories.

REFERENCES

[1] M. J. O'Neil, *The Merck Index*, 14th ed., Merck & Co., Inc., USA **2006**.

[2] *The United States Pharmacopoeia (USP 39)*, US Pharmacopoeia Convention, Inc., Rockville **2016**.

[3] L. L. Brunton, B. A. Chabner, B. C. Knollmann, *Goodman & Gilman's: The Pharmacological Basis of Therapeutics*, 12th ed., McGrew Hill Companies, Inc., China **2011**.

[4] S. C. Sweetman, P. S. Blake, *Martindale: The Complete Drug Reference*, 37th ed., Pharmaceutical Press, Italy **2011**.

[5] S. R. Narala, K. Saraswathi, *Int. J. Chem. Tech. Res.* **2011**, *3*, 605.

[6] A. M. Homoda, M. S. Kamel, K. Elmorsy, *J. Taibah Univ. Sci.* **2015**, *10*, 19.

[7] Y. Mrestani, R. Neubert, F. Nagel, *J. Pharm. Biomed. Anal.* **1999**, *20*, 899.

[8] A. Mendez, M. Steppe, E. Schapoval, *J. Pharm. Biomed. Anal.* **2003**, *33*, 947.

[9] N. A. Elragehy, E. M. Abdel-Moety, N. Y. Hassan, M. R. Rezk, *Talanta* **2008**, *77*, 28.

[10] B. C. McWhinney, C. W. Steven, T. Hillistera, A. R. Jason, P. J. Jacobus, *J. Chromatogr., B* **2010**, *878*, 2039.

[11] K. Kameda, K. Ikawa, K. Ikeda, N. Morikawa, *J. Chromatogr. Sci.* **2010**, *48*, 406.

[12] E. Dailly, R. Bouquié, P. Jolliet, R. Le Floch, *J. Chromatogr., B* **2011**, *879*, 1137.

[13] T. Ohmori, A. Suzuki, T. Niwa, H. Ushikoshi, K. Shirai, S. Yoshida, S. Ogura, Y. Itoh, *J. Chromatogr., B* **2011**, *879*, 1038.

[14] M. Zajac, J. Cielecka-Piontek, A. Jelinska, *Chem. Anal.* **2006**, *51*, 761.

[15] N. Y. Hassan, E. M. Abdel-Moety, N. A. Elragehy, M. R. Rezk, *Spectro. Chim. Acta A* **2009**, *72*, 915.

[16] N. A. Elragehy, N. Y. Hassan, M. R. Rezk, E. A. Moety, *J. Chromatogr. Sci.* **2010**, *48*, 624.

[17] K. Michalska, G. Pajchel, S. Tyski, *J. Chromatogr. A* **2009**, *1216*, 2934.

[18] M. Giancarlo, E. Elisa, F. Giocaliere Villanelli, S. Malvagiaa, S. Funghini, *J. Pharm. Biomed. Anal.* **2012**, *61*, 108.

[19] Y. W. Chou, Y. H. Yang, J. H. Chen, C. C. Kuo, S. H. Chen, *J. Chromatogr. B Anal. Technol.* **2007**, *856*, 294.

[20] A. Vailaya, P. Sajonz, O. Sudah, V. Capodanno, R. Helmy, F. D. Antia, *J. Chromatogr. A.* **2005**, *1079*, 80.

[21] P. Sajonz, A. Vailaya, O. Sudah, L. McPherson, V. Capodanno, T. K. Natishan, R. Helmy, F. D. Antia, *J. Chromatogr. A* **2006**, *1126*, 365.

[22] M. Zajac, J. Cielecka-Piontek, A. Jelinska, *Chem. Anal.* **2006**, *51*, 761.

[23] K. K. Jhankal, A. Sharma, Ramswaroop, D. K. Sharma, *IJPSR* **2015**, *6*, 3014.

[24] N. Y. Sreedhar, M. Sivaprasad, C. Swarupa, M. Dhananjayulu, M. R. Jayapal, *J. Anal. Bioanal. Tech.* **2014**, *5*, 192.

[25] M. Gumstas, N. Karadas, S. A. Ozkan, *Rev. Roum. Chim.* **2013**, *58(7–8)*, 679.

[26] D. Patra, A. K. Mishra, *TrAC, Trends Anal. Chem.* **2002**, *21*, 787.

[27] M. I. Walash, F. F. Belal, N. M. El-Enany, M. H. El-Maghrabey, *J. Chem. Cent.* **2011**, *5*, 70.

[28] M. K. Sharaf El-Din, F. A. Ibrahim, M. I. Eid, M. E. K. Wahba, *Acta Chim. Slov.* **2011**, *58*, 278.

[29] J. J. B. Nevado, J. A. M. Pulgarin, O. I. R. Escudero, *Appl. Spectrosc.* **2000**, *54*, 1678.

[30] G. L. Green, T. C. O'Haver, *Anal. Chem.* **1974**, *46*, 2191.

[31] P. John, I. Soutar, *Anal. Chem.* **1976**, *48*, 520.

[32] J. J. Santana Rodriguez, J. Hernandez, M. M. Bernal Suarez, A. Bermejo Martin-Lazaro, *Analyst* **1993**, *118*, 917.

[33] D. Patra, A. K. Mishra, *Talanta* **2001**, *53*, 783.

[34] D. Patra, T. H. Ghaddar, *Talanta* **2009**, *77*, 1549.

[35] L. I. Bebawy, K. El Kelani, L. Abdel Fattah, *J. Pharm. Biomed. Anal.* **2003**, *32*, 1219.

[36] J. Georges, *Analyst* **1993**, *118*, 1481.

[37] M. E. El-Kommos, G. A. Saleh, S. M. El-Gizawi, M. A. Abou-Elwafa, *Talanta* **2003**, *60*, 1033.

[38] A. G. Campaiia, F. Barrero, M. R. Ceba, *Anal. Chim. Acta* **1996**, *329*, 319.

[39] J. Karpinska, M. Kulikowska, *J. Pharm. Biomed. Anal.* **2002**, *29*, 153.

[40] K. A. Connors, *Binding Constants. The Measurements of Molecular Complex Stability*, Wiley, New York **1987**.

[41] J. Inczedy, *Analytical and Application of Complex Equilibria*, John Wiley and Sons Inc., Budapest **1976** 101.

[42] L. E. Abdel Fattah, T. A. Mohamed, E. A. Taha, *Chem. Ind. Chem. Eng. Q.* **2010**, *16*, 31.

[43] J. N. Miller, J. C. Miller, *Statistics and Chemometrics for Analytical Chemistry*, 6th ed., Pearson Education Limited, Harlow, England **2010**.

[44] *Guidance for Industry; Q2B of analytical procedure: Methodology*, International Conference on Hormonization (ICH), http://www.fda.gov/eder/guidance/1320fnl **2005**.

[45] *Product Specifications and Test Methods*, Merck Research Laboratories, Merck & Co., Inc., New Jersey **2009**.personal communication

[46] R. M. Youssif, Microanalysis of some of the novel non-classical β-lactams MSc Thesis, (Ain Shams University, Cairo, Egypt) **2013**.

How to cite this article: Elzanfaly ES, Youssif RM, Salama NN, Fayed AS, Hendawy HAM, Salem MY. Zero and second-derivative synchronous fluorescence spectroscopy for the quantification of two non-classical β-lactams in pharmaceutical vials: Application to stability studies. *Luminescence*. 2017;1–11. https://doi.org/10.1002/bio.3353